

# Assessment of weathering damage on the Petroglyphs of Cheonjeon-ri, Ulsan, Republic of Korea

Kurt Heinrichs · Bernd Fitzner

Received: 11 March 2010 / Accepted: 29 October 2010 / Published online: 16 November 2010  
© Springer-Verlag 2010

**Abstract** The Petroglyphs of Cheonjeon-ri in the area of Ulsan Metropolitan City in the southeastern part of the Republic of Korea represent outstanding cultural property of the country. The rock carvings—discovered about 40 years ago—provide valuable information on the life of the ancient people of different periods. In 1973, the petroglyphs were designated Korean National Treasure. Apparently, the petroglyphs have suffered damage from weathering such as loss of stone material, current detachment of stone material and deposits on the stone surface. The protection of this masterpiece of historic rock carving has become an important concern in the country. Geoscientific studies were carried out, targeted to stone analysis and to characterization and rating of weathering damage. The diagnostic studies combined laboratory analysis of representative unweathered and weathered stone material and in situ investigation by means of profile measurements at the carvings, mapping of weathering forms, ultrasonic measurements and rebound hardness measurements. Methodology and results of the material and damage diagnosis are presented. The results on type and extent of damage in combination with deduced risk prognosis reveal a considerable threat to the historical site of Cheonjeon-ri due to weathering and they indicate the need of intervention for monument preservation.

**Keywords** Petroglyphs · Petrographical studies · Weathering damage · Damage diagnosis · Risk prognosis · Republic of Korea

## Introduction

Petroglyphs (rock carvings) represent prominent examples of historic rock art. Compared to other countries, very few sites of petroglyphs are known from the Republic of Korea (petroglyphs here called “Amgakhwa”). Korea’s first petroglyphs were discovered in 1970/1971 such as the Bangudae Petroglyphs (situated at Daegok-ri, Eonyang-eup, Ulju-gun, Ulsan) and the Cheonjeon-ri Petroglyphs. In 2002, the International Symposium on the Conservation of the Bangudae Petroglyphs took place in Ulsan, Republic of Korea as a forum for discussing appropriate approaches to monument anamnesis, damage diagnosis and monument preservation (Kim 2002). On behalf of Ulsan Metropolitan City, the authors carried out studies on the Bangudae Petroglyphs in 2003. Evaluation and scientific rating of the weathering damage on the Bangudae Petroglyphs, the petrographical characterization of the rocks, risk prognosis and the deduction of information on need and urgency of preservation measures were the overall aims of these studies. Results have been presented in Fitzner et al. (2004). A considerable threat to the Bangudae Petroglyphs owing to weathering was stated, taking into consideration that the monument—since construction of the Sayeon dam in 1965—is submerged for about 8 months per year by the Sayeon reservoir.

In addition, the Cheonjeon-ri Petroglyphs were investigated. The Petroglyphs of Cheonjeon-ri (“Cheonjeollig-akseok”) are located in the southeastern part of the Republic of Korea at Dudong-myeon, Ulju-gun in the area

---

K. Heinrichs (✉)  
Department of Engineering Geology and Hydrogeology,  
RWTH Aachen University, Lochnerstraße 4-20,  
52064 Aachen, Germany  
e-mail: heinrichs@lih.rwth-aachen.de

B. Fitzner  
Geological Institute, RWTH Aachen University,  
Wüllnerstraße 2, 52062 Aachen, Germany

of Ulsan Metropolitan City, Gyeongsangbuk-do Province. In 1973, the Petroglyphs of Cheonjeon-ri were designated Korean National Treasure (No. 147). The petroglyphs are found on the smooth face of a rock cliff (about 9.5 m long and 2.7 m high; sedimentary rocks, probably of the Silla Series, Cretaceous) along the middle reaches of Naegokcheon Stream, one of the branches of the Taehwagang River in Ulsan City. The face of the rock cliff is exposed to SE, however inclines to NW (Fig. 1). The bedding planes of the rock incline with  $10^\circ$  in direction of WNW. The petroglyphs can be divided into two sections. The upper section dates from the Bronze Age. It was made by the techniques of Myeonjjogi (inside-chiseling) and Seonjjogi (outline-chiseling). The upper section features various abstract, geometrical designs (e.g. lozenges, circles) (Fig. 2) and images of animals (especially deers) and human beings. The lower section was made in the Silla Period (57 BC–935 AD) to memorialize a visit to this site by King Beopheung (514–540) and his queen. Along with carvings of animals and ships, it features cavalcade scenes in three places and, moreover, an inscription in more than 800 Chinese characters (Fig. 3), presumed to have been engraved on two occasions during the reign of King Beopheung (Cultural Heritage Administration of Korea, Yim, Van der Sluijs).

The Petroglyphs of Cheonjeon-ri show damage due to weathering. Irretrievable loss of stone material, current detachment of stone material and deposits on the stone surface are apparent. Moreover, the rock cliff is affected by a considerable number of structural discontinuities.

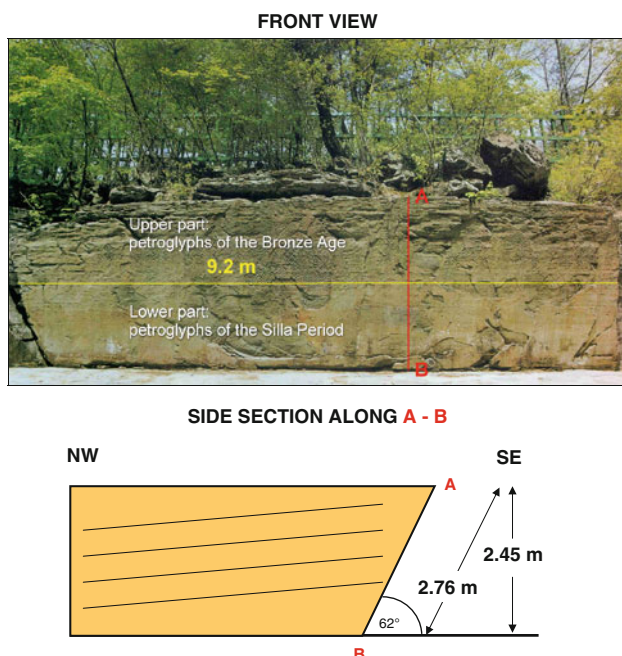


**Fig. 1** Petroglyphs of Cheonjeon-ri: front view and side section



**Fig. 2** Carvings of the Bronze Age



**Fig. 3** Carvings of the Silla Period

With respect to methodological approach, modern comprehensive diagnosis of weathering damage on stone monuments combines laboratory studies and in situ investigation procedures. Many different procedures have been developed and used over recent decades for in situ investigation of weathering damage. Nonetheless, there is no standardized methodological strategy for in situ assessment of visible or detectable weathering damage. Suitable methods are to be selected thoroughly each with a stone monument in accordance with the aims of investigation. Identification and evaluation of weathering forms has become an important part of in situ assessment of weathering damage (Smith et al. 1992; Mottershead 2000; Fitzner and Heinrichs 2002; Snethlage 2005; Prikryl 2007). Regarding the wide range of additional measuring techniques available for in situ investigation (e.g. Kownatzki 1997; Nappi and Côte 1997), preferably non-destructive procedures should be applied. In addition, operation mode, cost-effectiveness and quality of information output must be taken into account. With respect to diagnosis of weathering damage on the Cheonjeon-ri Petroglyphs, the diagnostical concept comprised laboratory analysis of representative unweathered and weathered rock and in situ

investigation by means of various experienced easy-to-perform, non-destructive and complementary measuring techniques along with mapping of weathering forms. The studies addressed evaluation and rating of the weathering damage on the Cheonjeon-ri Petroglyphs, characterization of rock properties and their substantial changes owing to weathering, risk prognosis and information on need of preservation measures.

**Methodological approach**

**In situ investigation**

In situ investigation of the Cheonjeon-ri Petroglyphs comprised profile measurements, monument mapping (mapping of weathering forms), rebound hardness measurements and ultrasonic measurements. The investigation areas are presented in Fig. 4. Profile measurements with a commercial profile comb were made at 30 petroglyphs of the Bronze Age for quantifying the morphological profile of the carvings (Fig. 5). The length of the measured sections amounted to 15 cm. The evaluation of results included graphic documentation of the profiles, determination of

maximum and average profile depths and the deduction of quantitative risk prognosis “future recession of the stone surface—corresponding percentage of carvings that will be completely lost”.

The monument mapping method was applied for the precise registration and documentation of all weathering forms affecting the stone surface. Weathering forms represent visible weathering phenomena at centimetre to metre scale. The standardized classification scheme of weathering forms by Fitzner and Heinrichs (2002) was used for mapping of weathering forms. It was adjusted to weathering forms identified on the monument. A suitable classification of their intensities was integrated. The registered weathering forms were illustrated in thematic maps “loss of stone material”, “discolouration/deposits”, “detachment of stone material”, “fissures” and were evaluated quantitatively. The results obtained from mapping of weathering forms were used for the identification of weathering progression phases.

Rebound hardness measurements were carried out with a Schmidt hammer (type PROCEQ LR, impact energy: 0.735 N m) at two representative investigation areas, each about 2 m<sup>2</sup> in size and with a rectangular grid of 63 measuring points arranged on the stone surface (Fig. 6). The registered rebound hardness values were classified according to minimum, maximum, average and class distribution, comparing carved and non-carved areas as well as different states of weathering.

Ultrasonic measurements were carried out with a STEINKAMP Ultrasonic Tester BPV (conic probes, 50 kHz) according to the refraction mode using the same grid of measuring points as for the rebound hardness measurements (Fig. 7). The horizontal and vertical distance between adjacent measuring points was 20 cm. Measurements were made along horizontal (*h*), vertical (*v*) and diagonal (two directions, *d1* and *d2*) measuring distances (Fig. 8). Evaluation of results included the

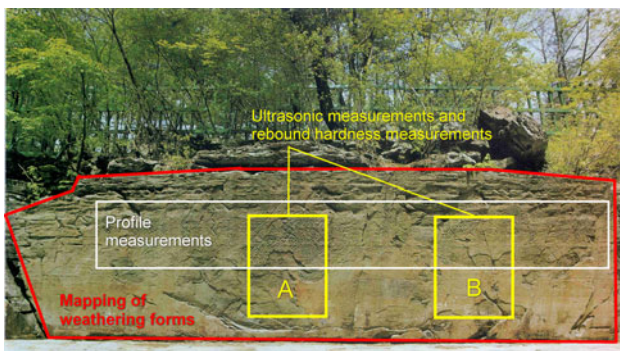


**Fig. 4** Investigation areas

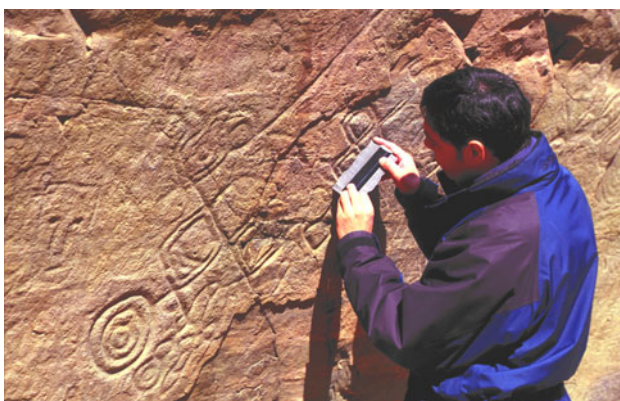


**Fig. 5** Profile measurements



**Fig. 6** Rebound hardness measurements with Schmidt hammer



**Fig. 7** Ultrasonic measurements

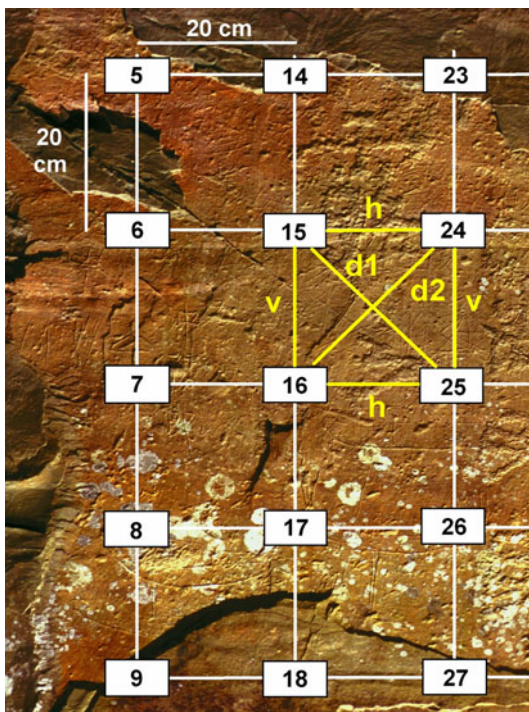


**Fig. 8** Grid of measuring points (section) at the investigation areas A and B for rebound hardness measurements and ultrasonic measurements (measurements: *h* horizontal; *v* vertical, *d1*, *d2* diagonal)

determination of ultrasonic velocities from measuring distance and registered transit time and the illustration of the ultrasonic velocities in maps by means of isolines. The maps of ultrasonic velocities were compared with the corresponding maps of weathering forms and structural discontinuities (fissures).

Damage categories were applied for the rating of the weathering forms with respect to degree of damage. Six damage categories were defined: 0, none; 1, very slight; 2, slight; 3, moderate; 4, severe; and 5, very severe. A correlation scheme “weathering forms, damage categories” was developed for the monument under investigation, in which all weathering forms—considering type and intensity—were related to damage categories. The high historic and artistic importance of the monument was taken into account. In addition, results obtained from the measurements on site (profile measurements, rebound hardness measurements, ultrasonic measurements) were considered. The damage categories were illustrated in maps and evaluated quantitatively. The quantitative evaluation of damage categories provided the basis for the calculation of damage indices as numerical parameters for overall quantification and rating of visible weathering damage on stone monuments (e.g. Fitzner and Heinrichs 2002; Fitzner et al. 2002; Heinrichs and Fitzner 2007; Heinrichs 2008). Additionally, the damage categories and damage indices were used for outlining vertical profiles of weathering damage on the Cheonjeon-ri monument.

#### Sampling, laboratory testing

Two representative stone samples—samples Cheonjeon-ri 1 (specimen,  $10 \times 6 \times 5$  cm) and Cheonjeon-ri 2 (specimen,  $8 \times 4 \times 4$  cm)—were collected from non-carved areas of the rock cliff for petrographical studies. Stone properties such as mineral composition, microtexture/structure, porosity properties, hygric properties and petrophysical properties were studied by means of X-ray diffraction, transmitted light microscopy with image analysis, scanning electron microscopy, mercury porosimetry, nitrogen adsorption method (BET), water absorption/desorption tests and ultrasonic measurements. Exemplarily, characteristic differences between unweathered and weathered stone were lined out for sample Cheonjeon-ri 1.

## Results

#### Petrography and petrophysical properties

The petrographical/petrophysical properties of the two stone samples (Cheonjeon-ri 1 and Cheonjeon-ri 2) are presented in the Tables 1, 2 and 3. The samples can be

**Table 1** Petrographical properties of the samples Cheonjeon-ri 1 and Cheonjeon-ri 2

	Cheonjeon-ri 1	Cheonjeon-ri 2
Mineral composition (%)		
Quartz	5.7	18.0
Feldspar	3.3	19.6
Rock fragments	8.5	9.7
Mica (grains)	0.6	2.2
Chlorite (grains)	0.1	0.7
Matrix: micrite, clay minerals, micro-quartz	75.2	39.5
Matrix: sparite	5.8	5.9
Matrix: opaque matter	0.8	4.3
Petrographic classification according to Pettijohn et al. (1987)	Mudstone	Feldspathic greywacke
Matrix–grain relation		
Matrix–grain ratio	4.49	0.99
Fabric	Matrix-supported	Matrix-supported
Grain size characteristics		
Mean grain size <i>M</i> (μm) according to Trask (in Tucker 1988)	45.5	49.9
Sorting <i>S</i> <sub>o</sub> according to Trask (in Tucker 1988)	1.23 (very well sorted/ well sorted)	1.26 (well sorted)
Grain size distribution (%) (Wentworth classification)		
Coarse silt (31–63 μm)	84.6	76.5
Very fine sand (63–125 μm)	14.3	17.6
Fine sand (125–250 μm)	0.7	4.3
Medium sand (250–500 μm)	0.4	1.1
Coarse sand (500–1,000 μm)	–	0.5

**Table 2** Petrographical properties of the samples Cheonjeon-ri 1 and Cheonjeon-ri 2

	Cheonjeon-ri 1		Cheonjeon-ri 2
	Unweathered	Weathered	
Porosity properties			
Density (g/cm <sup>3</sup> )	2.69	2.68	2.69
Bulk density (g/cm <sup>3</sup> )	2.66	2.29	2.65
Total porosity (vol.%)	1.2	14.7	1.4
Porosity: micropores radii ≤ 0.1 μm (vol.%)	0.2	1.1	0.4
Porosity: capillary pores radii > 0.1 μm (vol.%)	1.0	13.6	1.0
Mean radius of pore entries (μm)	0.01	0.05	0.01
Pore surface (m <sup>2</sup> /g)	0.80	2.23	0.99
Pore surface (m <sup>2</sup> /cm <sup>3</sup> )	2.13	5.11	2.62

described as clayish-silty, compact stone of greyish colour. Sample Cheonjeon-ri 1 shows a marginal whitish-brownish weathered zone (Fig. 9). The thickness of this weathered zone ranges between 0.1 and 1 cm. The samples are composed of quartz, feldspar (albite, microcline), rock fragments, mica (especially muscovite), chlorite and matrix (Table 1). The matrix is composed of clay minerals (chlorite, muscovite/sericite), carbonate (micritic and sparitic calcite), opaque matter (hematite) and micro-quartz. Comparing the samples, Cheonjeon-ri 2 shows higher contents of quartz and feldspar, whereas the content of matrix relating to micrite, clay minerals and micro-quartz

is correspondingly lower. Comparing unweathered and weathered parts of sample Cheonjeon-ri 1, loss of carbonate (calcite) in the weathered part is the most striking characteristic (Fig. 10). According to the petrographical classification of Pettijohn et al. (1987), Cheonjeon-ri 1 is to be classified as “mudstone”, Cheonjeon-ri 2 as “feldspathic greywacke”.

The matrix–grain ratio ranges from 4.49 (Cheonjeon-ri 1) to 0.99 (Cheonjeon-ri 2). Both samples are characterized by matrix-supported fabric with grains of quartz, feldspar, rock fragments, mica and chlorite mainly floating in the matrix. Direct contacts of grains are rare. In both samples,

**Table 3** Petrographical/ petrophysical properties of the samples Cheonjeon-ri 1 and Cheonjeon-ri 2

	Cheonjeon-ri 1	Cheonjeon-ri 2
Hygric properties		
Water absorption		
Water uptake at atmospheric pressure (wt%)	0.46	0.47
Water uptake at pressure, 150 bar (wt%)	0.64	0.52
Saturation coefficient	0.98	0.90
Water desorption		
Rest water content in relation to water absorption at atmospheric pressure (%)	40.3	22.2
Rest water content in relation to water absorption at pressure (%)	39.7	20.0
Petrophysical properties		
Ultrasonic velocity (m/s)		
Parallel to bedding (a)	4,984	4,480
Perpendicular to bedding (b)	4430	3842
Anisotropy index = (a):(b)	1.13	1.17

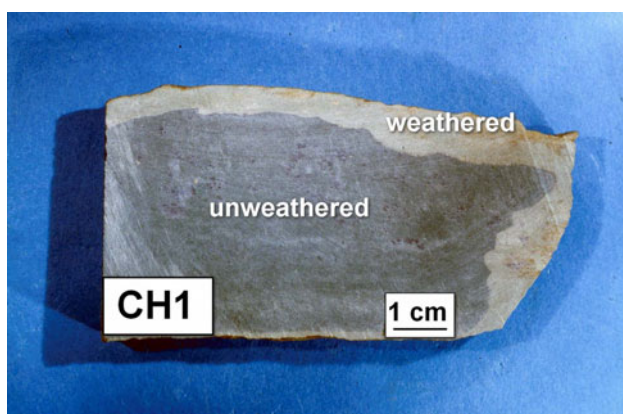


**Fig. 9** Sample Cheonjeon-ri 1: unweathered/weathered

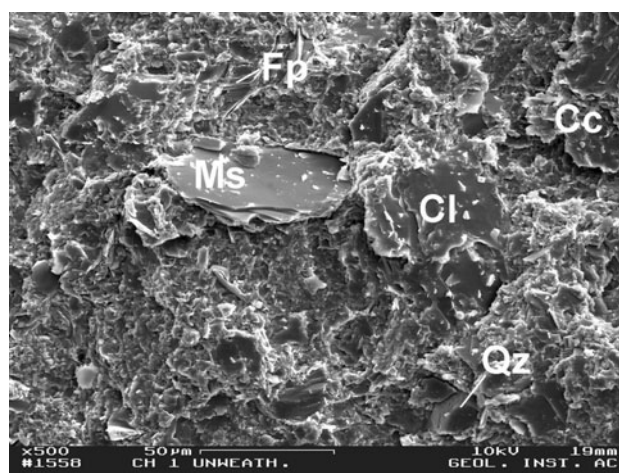


**Fig. 11** Sample Cheonjeon-ri 1: unweathered. SEM micrograph, image width: 0.23 mm. *Qz* quartz, *Fp* feldspar, *Ms* muscovite, *Cl* chlorite, *Cc* sparitic calcite

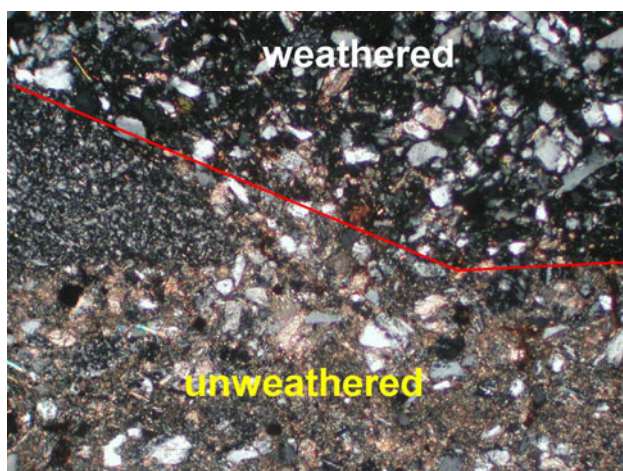


**Fig. 10** Sample Cheonjeon-ri 1: unweathered/weathered. Transmitted light microscopy, +Nic. Image width: 1.29 mm

most of the grains (components with a diameter > 30 μm considered as grains) occur in the class of coarse silt. The mean grain size (according to Trask, in Tucker 1988) ranges from 45.5 μm (Cheonjeon-ri 1) to 49.9 μm (Cheonjeon-ri 2). Comparing the samples, Cheonjeon-ri shows higher portions of very fine sand, fine sand, medium sand and coarse sand than Cheonjeon-ri 1 (considering grain size classes according to Wentworth). According to Trask in Tucker (1988), Cheonjeon-ri 1 is to be classified as “very well to well sorted”, Cheonjeon-ri 2 as “well-sorted”.

The unweathered parts of the two samples are characterized by very low total porosity (Table 2). Pore sizes are mainly in the range of smaller capillary pores. The pores are characterized by very small pore entries. The pore surface is rather high. Comparing the unweathered and

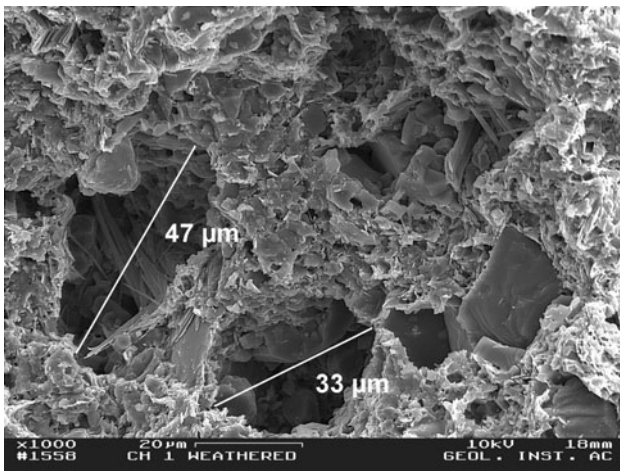


**Fig. 12** Sample Cheonjeon-ri 1: weathered. SEM micrograph, image width: 0.11 mm. Pores due to weathering

weathered part of sample Cheonjeon-ri 1, the weathered part shows a significantly higher total porosity, mainly resulting from increase of capillary pores due to the dissolution of the carbonate components, especially sparite (Figs. 11, 12). The pore surface in the weathered part of the sample is higher than in the unweathered part.

As result of the low porosity, water absorption of the unweathered samples is low (Table 3). However, the ratio between water absorption at atmospheric pressure and water absorption at pressure (here: 150 bar)—expressed by the saturation coefficient (Hirschwald 1908)—is very high. Water absorption and water desorption of the samples take place very slowly. Especially, Cheonjeon-ri 1 shows a rather high water retention. 40% of water remains in the stone after the drying test (duration: 7 days; conditions: 20°C, 50% rel. humidity). With respect to Cheonjeon-ri 1, it was not possible to investigate water absorption and desorption of the weathered part of the sample. From the porosity properties, it can be expected that water absorption in the weathered part is considerably higher than in the unweathered part, whereas degree of water saturation and rest water content after drying are lower.

The ultrasonic velocities are rather high for sedimentary rocks and reflect a high compactness/hardness of the stone. The ultrasonic velocities parallel to bedding are significantly higher than those perpendicular to bedding. This indicates a considerable anisotropic character of the stone material. Lower ultrasonic velocities—indicating decrease of compactness/hardness—can be expected for the weathered part of Cheonjeon-ri 1.

**Weathering forms**

The weathering forms that were found on the Cheonjeon-ri monument can be attributed to four groups of weathering

forms: “loss of stone material” (with five individual weathering forms), “discolouration/deposits” (with four individual weathering forms), “detachment of stone material” (with ten individual weathering forms) and “fissures” (with two individual weathering forms). In all, 21 individual weathering forms were stated with additional variation of intensities. Some characteristic weathering forms are shown in Fig. 13. The map of weathering forms relating to “loss of stone material” is presented in Fig. 14. 64.5% of the stone surface under investigation has already suffered loss of stone material. The following weathering forms were identified: “back weathering”, “relief” and “break out” (Table 4).

“Colouration”, “soiling by particles from the atmosphere or from water”, “coloured crust tracing the surface” and “microbiological colonization” were found as weathering forms with respect to “discolouration/deposits” (Table 5).

Ten individual weathering forms relating to “detachment of stone material” were identified, in all affecting 42.1% of the stone surface under investigation (Fig. 15; Table 6): “crumbling”, “single flakes”, “multiple flakes”, “single scale”, “multiple scales”, “splitting up”, “single flakes–crumbling” (transitional form), “crumbling–single

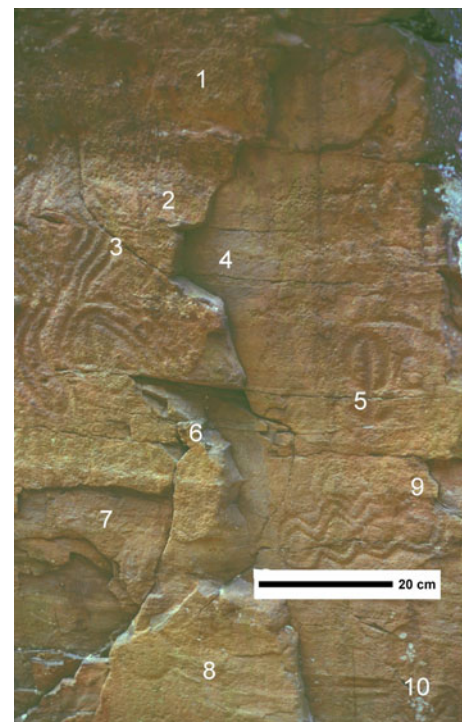


**Fig. 13** Weathering forms. 1 soiling, 2 crumbling–single scale, 3 fissure independent of stone structure, 4 break out, 5 fissure dependent on stone structure, 6 crumbling, 7 back weathering due to loss of scales, multiple scales, 8 crust, 9 single scale, 10 microbiological colonization

**Fig. 14** Map and quantitative evaluation (area%) of weathering forms relating to “loss of stone material”

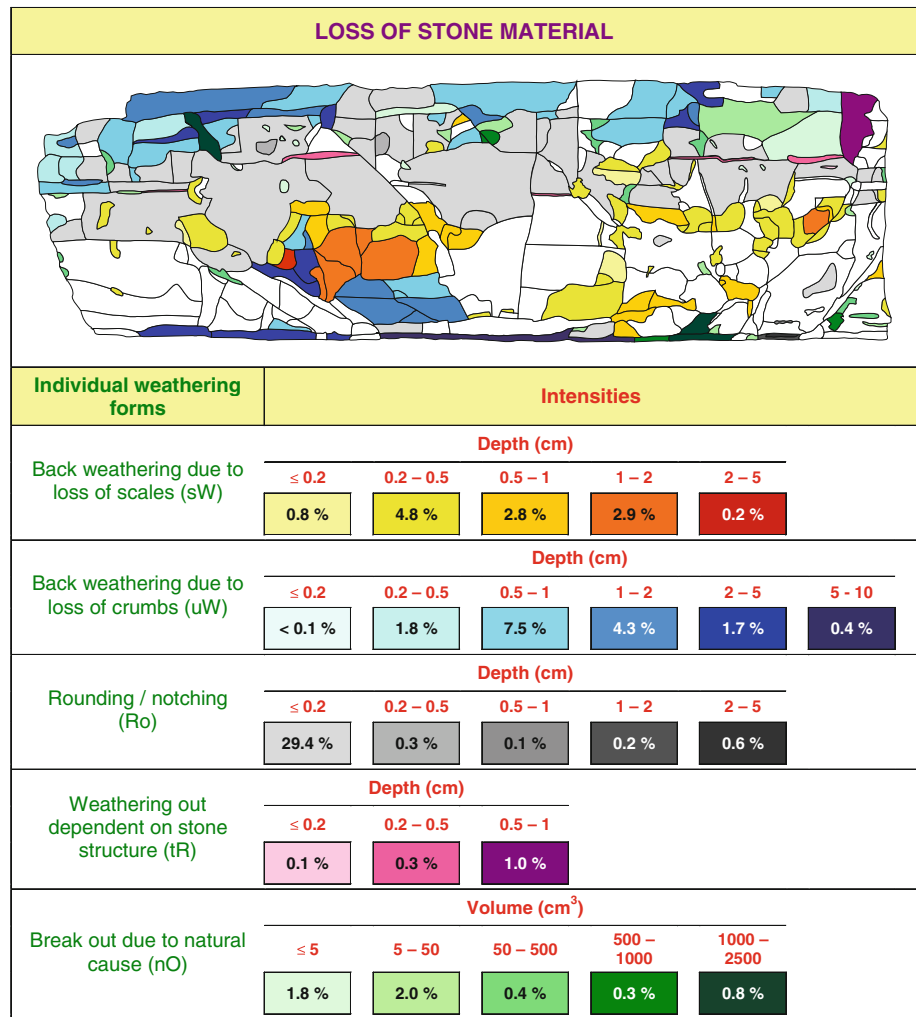


**Table 4** Weathering forms relating to “loss of stone material”

Weathering forms (stone surface affected, area%)	Comments
“Back weathering”: uniform loss of stone material parallel to the original stone surface (27.2%)	
“Back weathering due to loss of scales” (11.5%)	Depth of back weathering mainly in the range between 0.2 and 2 cm; back weathering due to crumbs mainly limited to the uppermost and lowermost parts of the monument;
“Back weathering due to loss of crumbs” (15.7%)	back weathering due to loss of scales mainly on the middle to lower part of the monument
“Relief”: morphological change of the stone surface due to partial or selective weathering (32.0%)	
“Rounding/notching” (30.6%)	Both individual weathering forms mainly on the middle to upper part of the investigation area; depth of relief formation ≤0.2 cm (lowest intensity) prevalent
“Weathering out dependent on stone structure” (1.4%)	
“Break out”: loss of compact stone fragments (5.3%)	Mainly in the uppermost and lowermost parts of the investigation areas and here often along fissures; dimension of missing parts mainly amounting to less than 50 cm <sup>3</sup>



**Table 5** Weathering forms relating to “discolouration/deposits”

Weathering forms (stone surface affected, area%)	Comments
“Colouration”: here brownish-reddish colouration, probably due to precipitation of Fe compounds (3.8%)	Mainly in the lowermost part of the investigation area
“Soiling by particles from the atmosphere or from water”: poorly adhesive deposits on the stone surface; here mainly brownish deposits of dust, soil or mud particles (98.6%)	Distributed all over the stone surface
“Coloured crust tracing the surface”: compact, strongly adhesive deposits on the stone surface, tracing the morphology of the stone surface; here brownish thin crust; on (91.0%)	Distributed all over the stone surface
“Microbiological colonization”: colonization by micro-organisms/ biofilms (36.6%)	Mainly limited to the uppermost and lower parts of the investigation area; intense microbiological colonization mainly on the lowermost part of the monument

**Fig. 15** Maps and quantitative evaluation (area%) of weathering forms relating to “detachment of stone material”

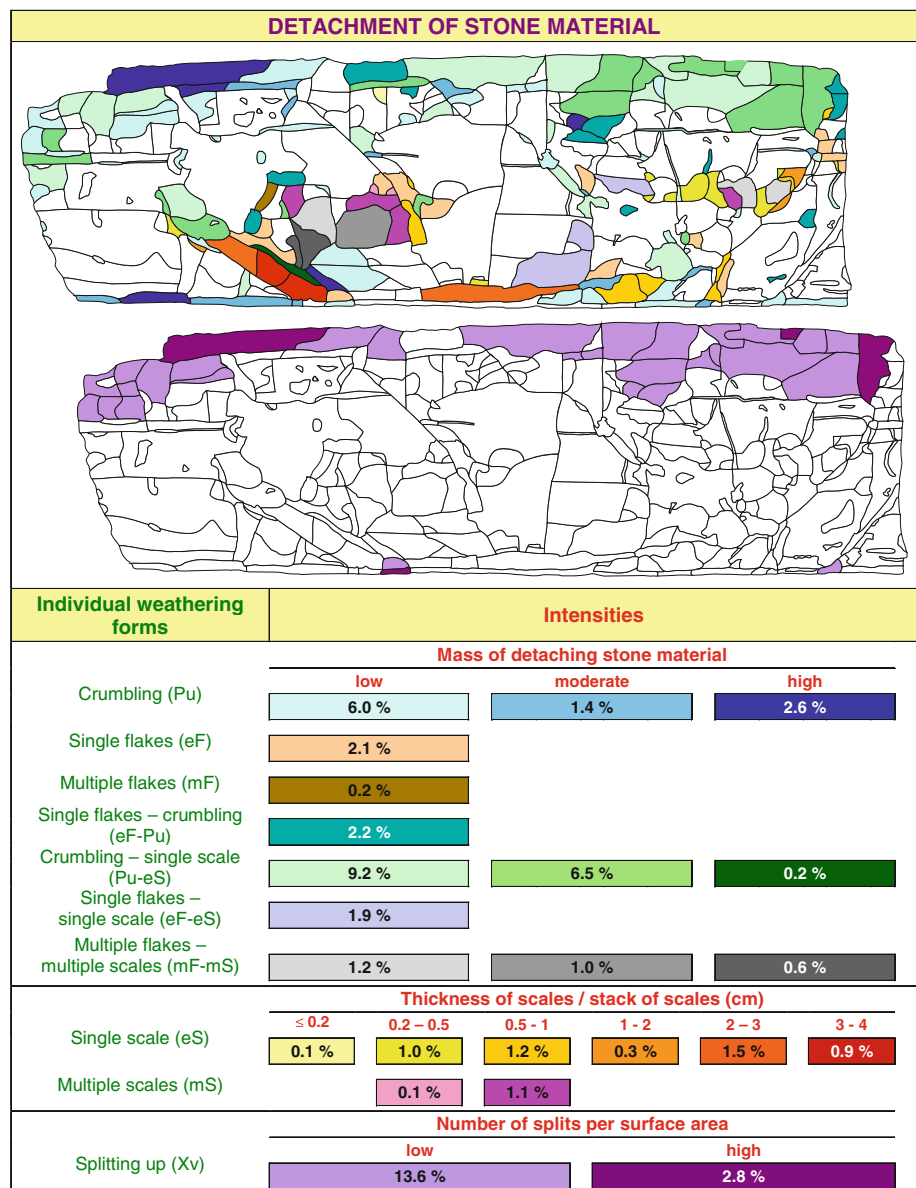


**Table 6** Weathering forms relating to “detachment of stone material”

Weathering forms (stone surface affected, area%)	Comments
“Crumbling”: detachment of larger more or less compact stone pieces of irregular shape (crumbs) (10%)	Low intensity (mass of detaching stone material: low) prevalent, mainly limited to the uppermost and lowermost parts of the monument
“Single flakes”: detachment of one layer of small, thin stone pieces (flakes) parallel to the stone surface (2.1%)	Only low intensity (mass of detaching stone material: low), mainly on the middle part of the investigation area (regarding height), mainly on parts of the stone surface that have already suffered “back weathering due to loss of scales”
“Multiple flakes”: detachment of a stack of small, thin stone pieces (flakes) parallel to the stone surface (0.2%)	Only low intensity (mass of detaching stone material: low), occurring on the middle part of the investigation area on a part of the stone surface that has already suffered “back weathering due to loss of scales”
“Single scale”: detachment of one layer of larger, platy stone pieces (scales) parallel to the stone surface (5.0%)	Six intensities, mainly on the lower part of the monument, mainly on parts of the stone surface that have not suffered any loss of stone material yet, otherwise on parts of the stone surface that have already suffered “back weathering due to loss of scales”
“Multiple scales”: detachment of a stack of larger, platy stone pieces (scales) parallel to the stone surface (1.2%)	Two intensities, higher intensity (thickness of the stack of scales: 0.5–1 cm) prevalent, only occurring on stone surface in the middle part of the monument that has already suffered “back weathering due to loss of scales”
“Splitting up”: detachment of larger stone layers (sheets, plates) following the stone structure (bedding) (16.4%)	Often in combination with “crumbling” or “crumbling–single scale”, low intensity prevalent, almost limited to the uppermost part of the monument
“Single flakes–crumbling”: transitional form between “single flakes” and “crumbling” (2.2%)	Only low intensity (mass of detaching stone material: low), mainly on stone surface in the upper part of the monument
“Crumbling–single scale”: transitional form between “crumbling” and “single scale” (15.9%)	Mostly in combination with “splitting up”, three intensities, low and moderate intensity (mass of detaching stone material: low, moderate) prevalent, occurrence mainly on the uppermost part of the monument
“Single flakes–single scale”: transitional form between “single flakes” and “single scale” (1.9%)	Only low intensity (mass of detaching stone material: low), only on parts of the stone surface that have already suffered “back weathering due to loss of scales”, occurrence on the middle and lower part of the investigation area
“Multiple flakes–multiple scales”: transitional form between “multiple flakes” and “multiple scales” (2.8%)	Three intensities, low and moderate intensity (mass of detaching stone material: low, moderate) prevalent, only on stone surface in the middle part of the monument that has already suffered “back weathering due to loss of scales”

scale” (transitional form), “single flakes–single scale” (transitional form) and “multiple flakes–multiple scales” (transitional form).

The map of “fissures” is presented in Fig. 16. Two intensities were distinguished according to opening width of the fissures. In all, 67 fissures were stated. “Fissures independent of stone structure”—distributed all over the investigation area—are prevalent. “Fissures dependent on

stone structure” mainly concern the upper part of the monument. Quantitative evaluation of the fissures has provided the following results:

- “Fissures independent of stone structure”, intensity 1 (opening width: narrow, mm-range): 37 fissures, total length of all fissures: 19 m; maximum length, individual fissure: 1.6 m; average length of fissures: 0.5 m.

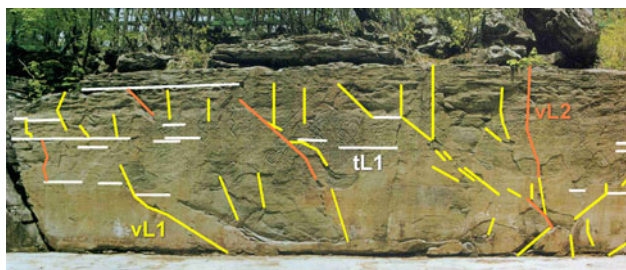


**Fig. 16** Map of fissures. *tL1* fissures dependent on stone structure, intensity 1; *vL1* fissures independent of stone structure, intensity 1; *vL2* fissures independent of stone structure, intensity 2

- “Fissures independent of stone structure”, intensity 2 (opening width: wide, cm-range): 5 fissures, total length of all fissures: 5 m; maximum length, individual fissure: 2.0 m; average length of fissures: 1 m.
- “Fissures dependent on stone structure”, only intensity 1 (opening width: narrow, mm-range): 25 fissures, total

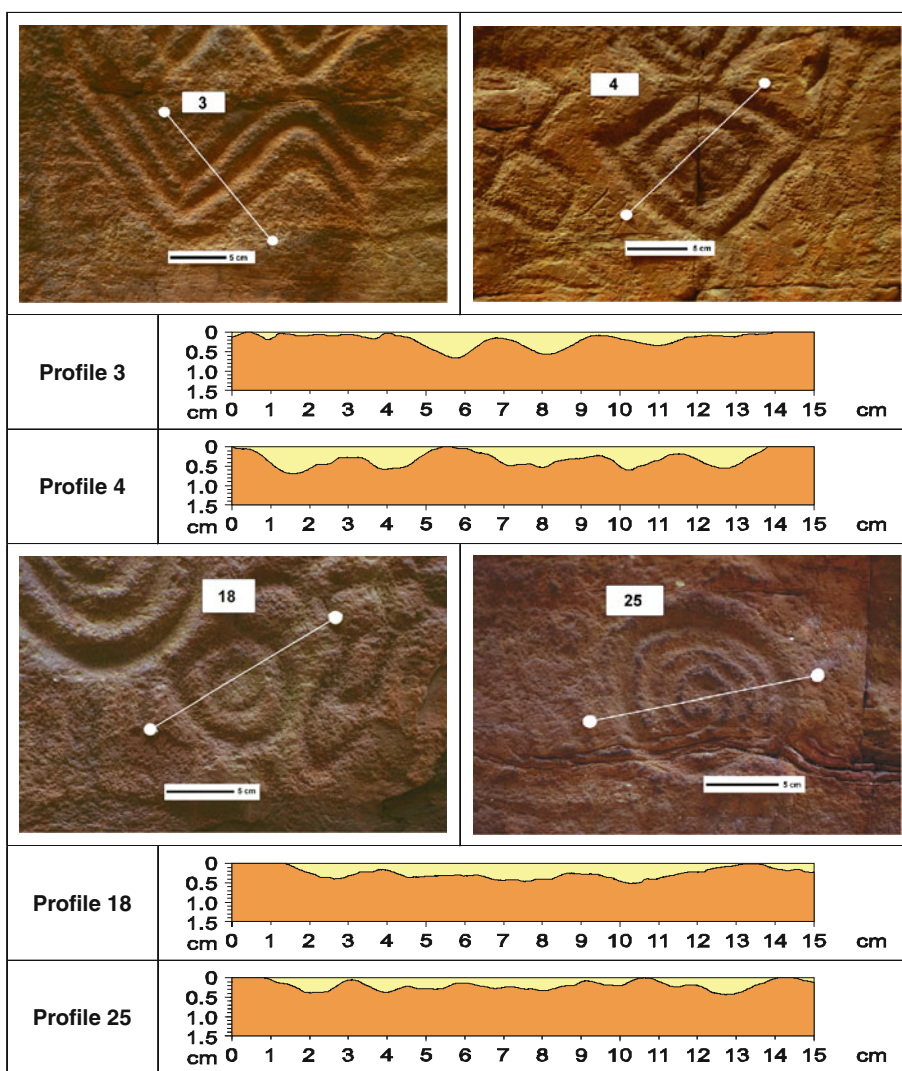
length of all fissures: 13 m; maximum length, individual fissure: 2.2 m; average length of fissures: 0.5 m; mainly in the upper part of the monument.

**Results of the in situ measurements**

The profile measurements at 30 carvings of the Bronze Age statistically distributed all over the upper part of the monument have shown that the maximum depth of the carvings ranges between 2.9 and 9.8 mm (Figs. 17, 18). The maximum profile depth of 70% of the carvings is in the range between 4 and 7 mm. The average profile depth of the carvings was found to be mainly in the range between 1 and 4 mm.

The distribution of the registered rebound hardness values is presented in Fig. 19. The rebound hardnesses range between 26 and 58 (investigation area A; average rebound hardness 45), respectively, between 30 and 60 (investigation area B; average rebound hardness 44).

**Fig. 17** Profile measurements at carvings of the Bronze Age: examples



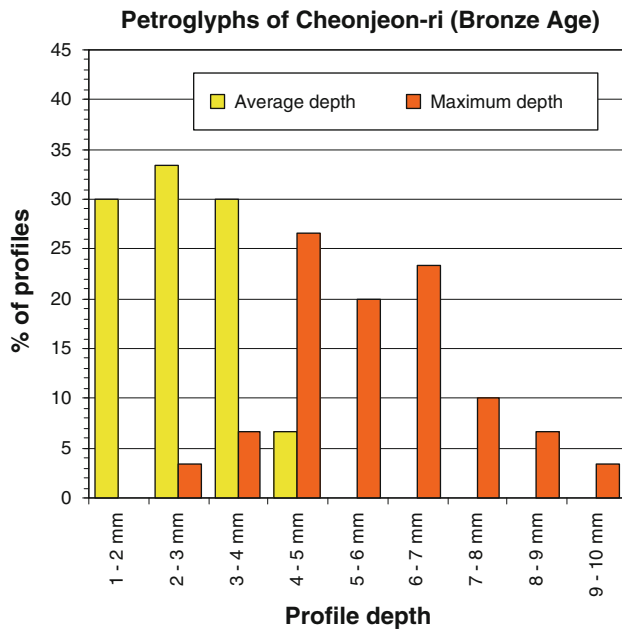


**Fig. 18** Profile measurements at carvings of the Bronze Age. Classification of average and maximum depths

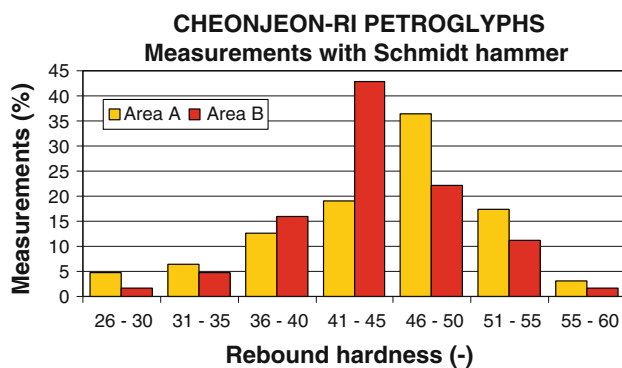


**Fig. 19** Classification of rebound hardnesses (investigation areas A and B)

Figure 20 shows a more detailed evaluation of the data in consideration of different states of weathering. The rebound hardness for non-carved areas without any visible loss and current detachment of stone material is in the range between 43 and 60 (average 49). It is striking that the rebound hardness for the carved areas (petroglyphs) without any visible stone deterioration is significantly lower. It ranges between 38 and 46 (average 41). Stone surface that has suffered loss of stone material due to prior detachment of stone material and that currently is not re-affected by detachment of stone material shows rebound hardnesses (range 40–57, average 48) almost as high as stated for non-carved areas without any visible loss and current detachment of stone material.

Results of the ultrasonic measurements are presented in Figs. 21, 22, and 23. First, isoline illustrations were made separately for the ultrasonic velocities derived from horizontal, vertical and diagonal ( $d_1$ ,  $d_2$ ) measurements (shown for investigation area A in Fig. 24 as example). In a next step, isoline illustrations were prepared regarding average ultrasonic velocities (jointly considering results from horizontal, vertical and diagonal measurements) and regarding minimum ultrasonic velocities (jointly considering minima from horizontal, vertical and diagonal measurements). These are presented in Fig. 21 (investigation area A) and Fig. 23 (investigation area B) in combination with the corresponding maps of fissures and the weathering forms characterizing current detachment of stone material.

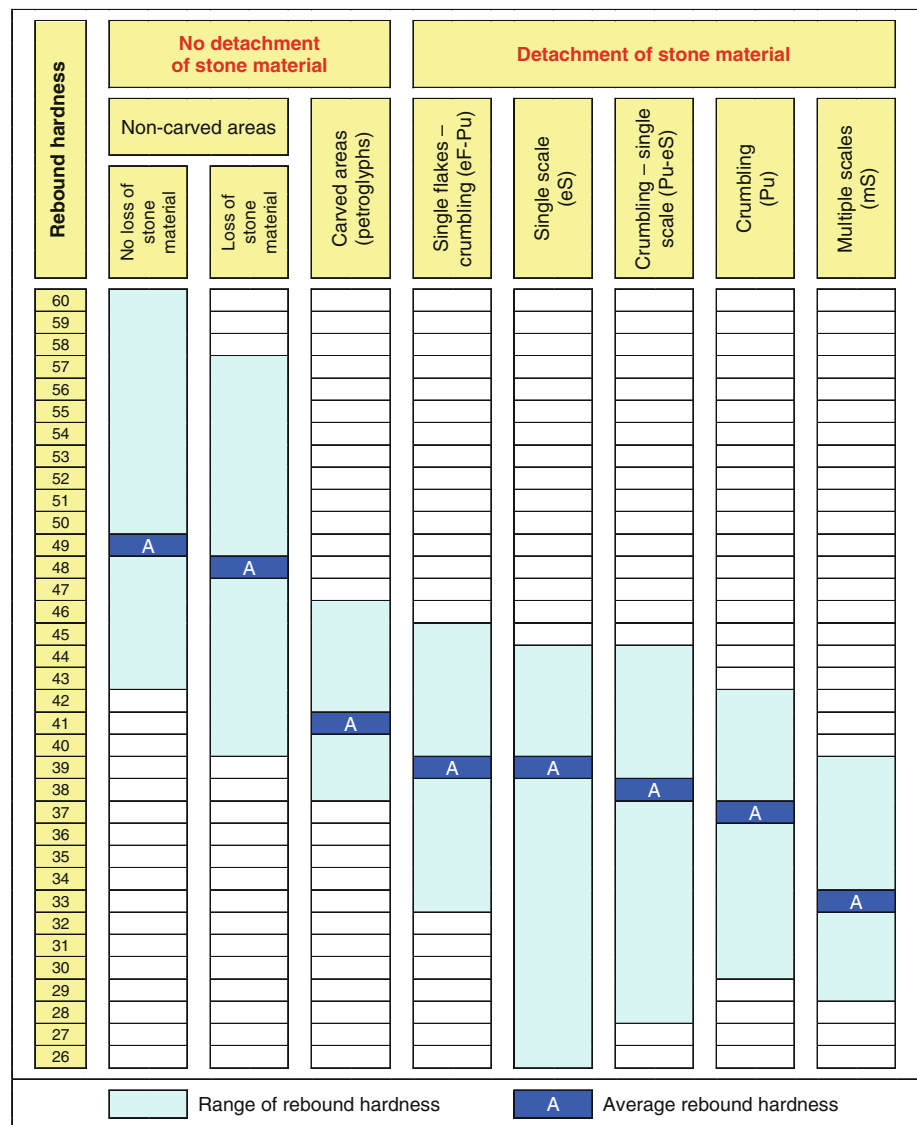
Maximum ultrasonic velocities (class: 4.500–4.750 m/s) correspond to the ultrasonic velocities determined for the unweathered parts of the stone samples under investigation. Low ultrasonic velocities clearly trace:

- the fissures, here especially the fissures independent of stone structure; ultrasonic velocities decrease as dimension—depth and/or width—of the fissures increases; very low ultrasonic velocities especially derived from horizontal and diagonal/ $d_2$  measurements,
- the various types of stone detachment, especially “single scale”, “multiple scales”, “crumbling” and “crumbling—single scale”.

#### Damage categories, damage index

The correlation scheme “weathering forms—damage categories”—specially developed for the Cheonjeon-ri Petroglyphs—is presented in Fig. 24. Based on this correlation scheme, damage categories were determined separately for loss of stone material, discolouration/deposits and detachment of stone material. Final damage categories were derived by jointly considering loss of stone material, discolouration/deposits and detachment of stone material according to the scheme presented in Fig. 25. The calculation of the damage index is based on the quantitative evaluation of the damage categories (Fig. 26). The damage index corresponds to “average damage category”. The individual maps of damage categories relating to loss of stone material, discolouration/deposits and detachment of stone material with corresponding quantitative evaluation of damage categories and determination of the damage index are presented in Fig. 27. The map of final damage categories—jointly considering loss of stone material, discolouration/deposits and detachment of stone material—with quantitative evaluation and determination of the damage index is shown in Fig. 28. Based on the four maps of damage

**Fig. 20** Range and average of rebound hardnesses in dependence on state of weathering



categories, vertical damage index profiles relating to loss of stone material, discolouration/deposits, detachment of stone material and total damage were derived for the entire monument from height-wise analysis of horizontal sections (Fig. 29). Results on damage categories and damage index can be summarized as follows:

Upper part with carvings of the Bronze Age

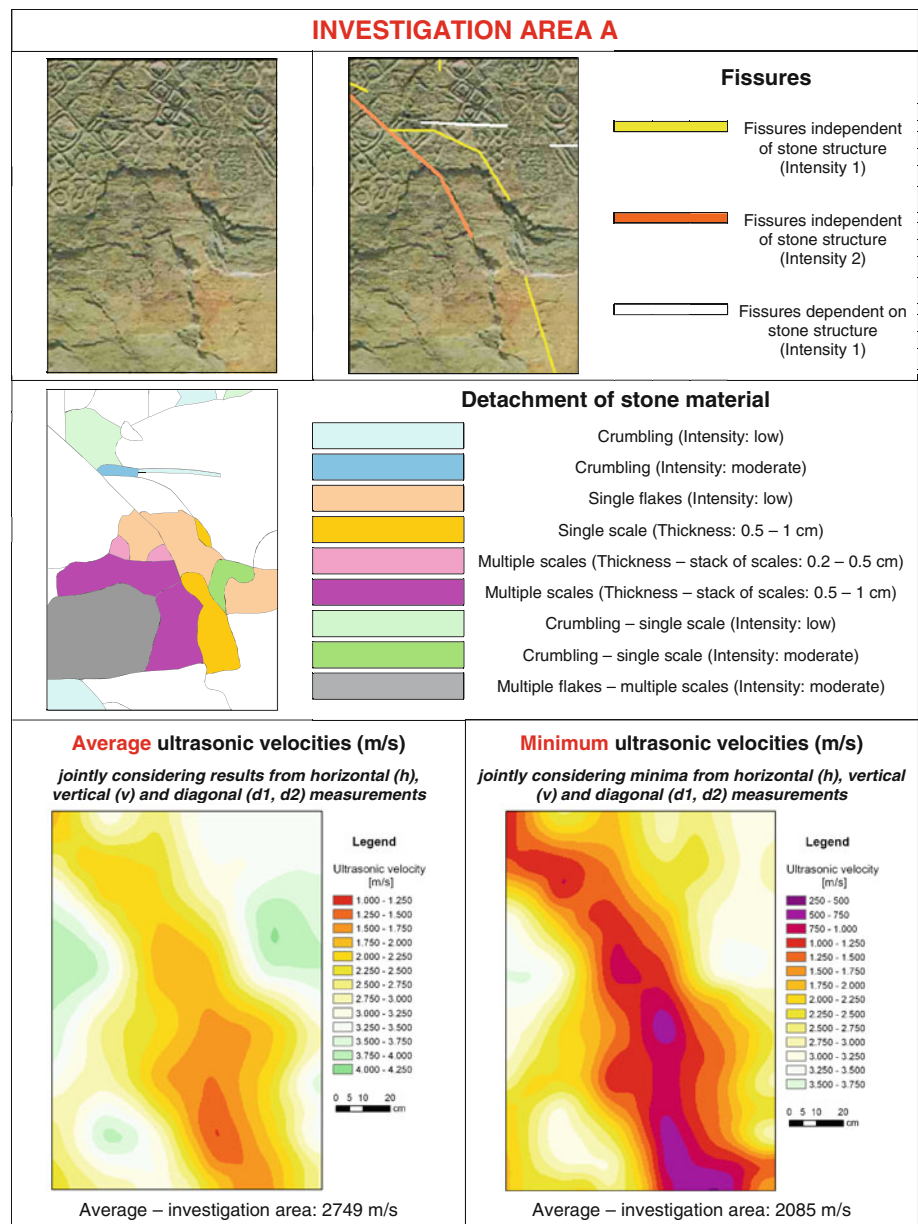
- with respect to loss of stone material: mainly severe damage; very severe damage in the uppermost part,
- with respect to discolouration/deposits: mainly very slight damage,
- with respect to detachment of stone material: larger parts of the stone surface without visible damage; mainly moderate or severe damage in the uppermost part,

- with respect to total damage (jointly considering loss of stone material, discolouration/deposits and detachment of stone material): mainly severe damage; very severe damage prevalent in the uppermost part.

Lower part with carvings of the Silla Period

- with respect to loss of stone material: most of the stone surface without visible damage; very severe damage in the lowermost part and in a middle to left part,
- with respect to discolouration/deposits: mainly very slight damage; slight damage prevalent in the lowermost part,
- with respect to detachment of stone material: larger parts of the stone surface without visible damage; moderate to very severe damage in the lowermost

**Fig. 21** Investigation area A: maps of average and minimum ultrasonic velocities. In addition, corresponding maps of fissures and weathering forms relating to current detachment of stone material



part; irregular distribution of parts with slight, moderate, severe or even very severe damage,

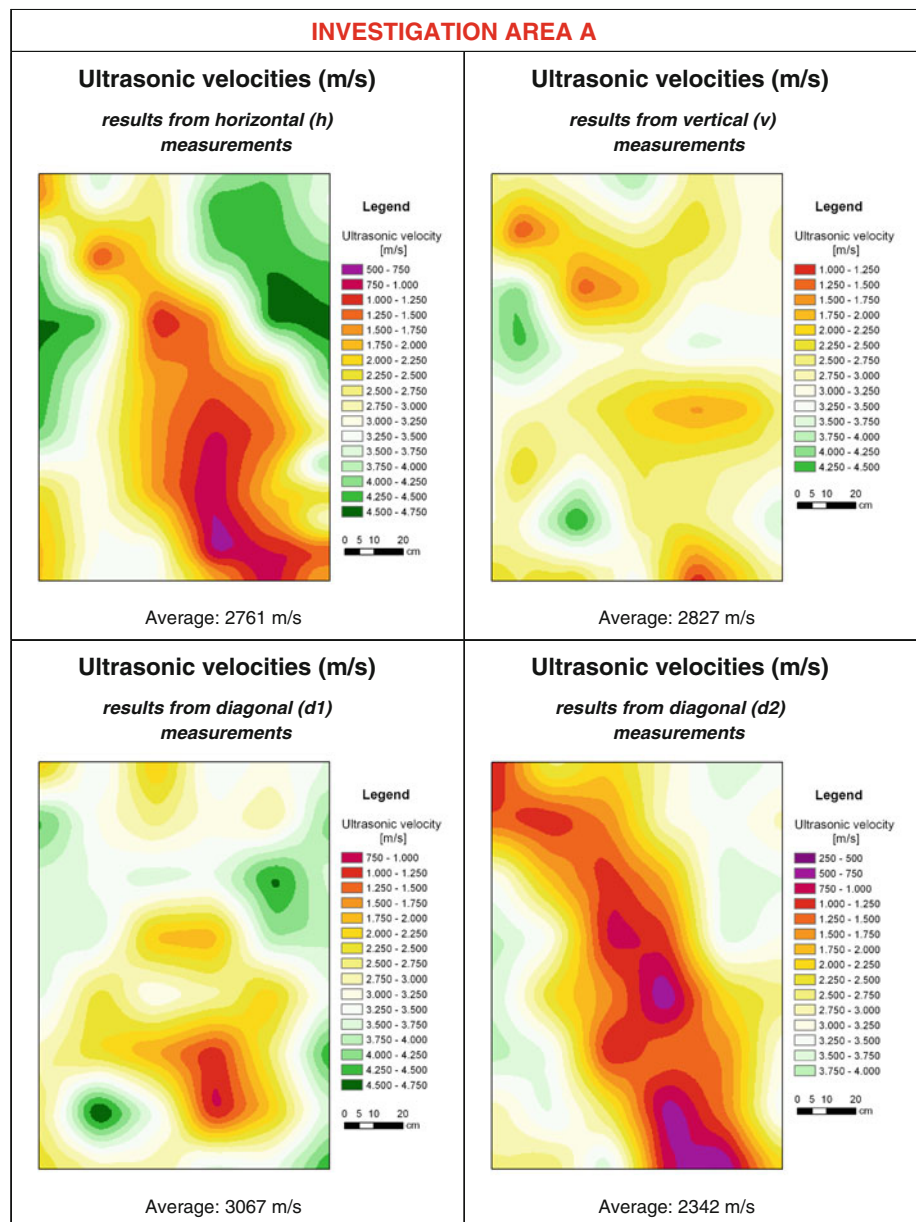
- with respect to total damage (jointly considering loss of stone material, discolouration/deposits and detachment of stone material): very severe damage in the lowermost part and in a middle to left part; remaining parts mainly with very slight damage or slight damage.

## Discussion

According to the results obtained from laboratory analysis, the Cheonjeon-ri Petroglyphs were carved from compact,

silty, carbonatic mudstones/greywackes, which—in unweathered state—are characterized by very low porosity and low water absorption capacity. The most striking characteristic of the weathered stone is dissolution of carbonate (chemical decomposition) resulting in increase of porosity and water absorption capacity and decrease of compactness/hardness. Considering the results on porosity characteristics and water absorption/desorption behaviour, it can be assumed that the stone retains a considerable water content even in dry season. Furthermore, it can be assumed for this stone material that wetting/drying cycles are accompanied by considerable swelling/shrinking processes (physical disintegration). However, due to the lack of sufficient information on environmental conditions in the area of the petroglyphs, reliable

**Fig. 22** Investigation area A: maps of ultrasonic velocities; results from horizontal, vertical and diagonal measurements



information on weathering factors and weathering processes is not possible yet.

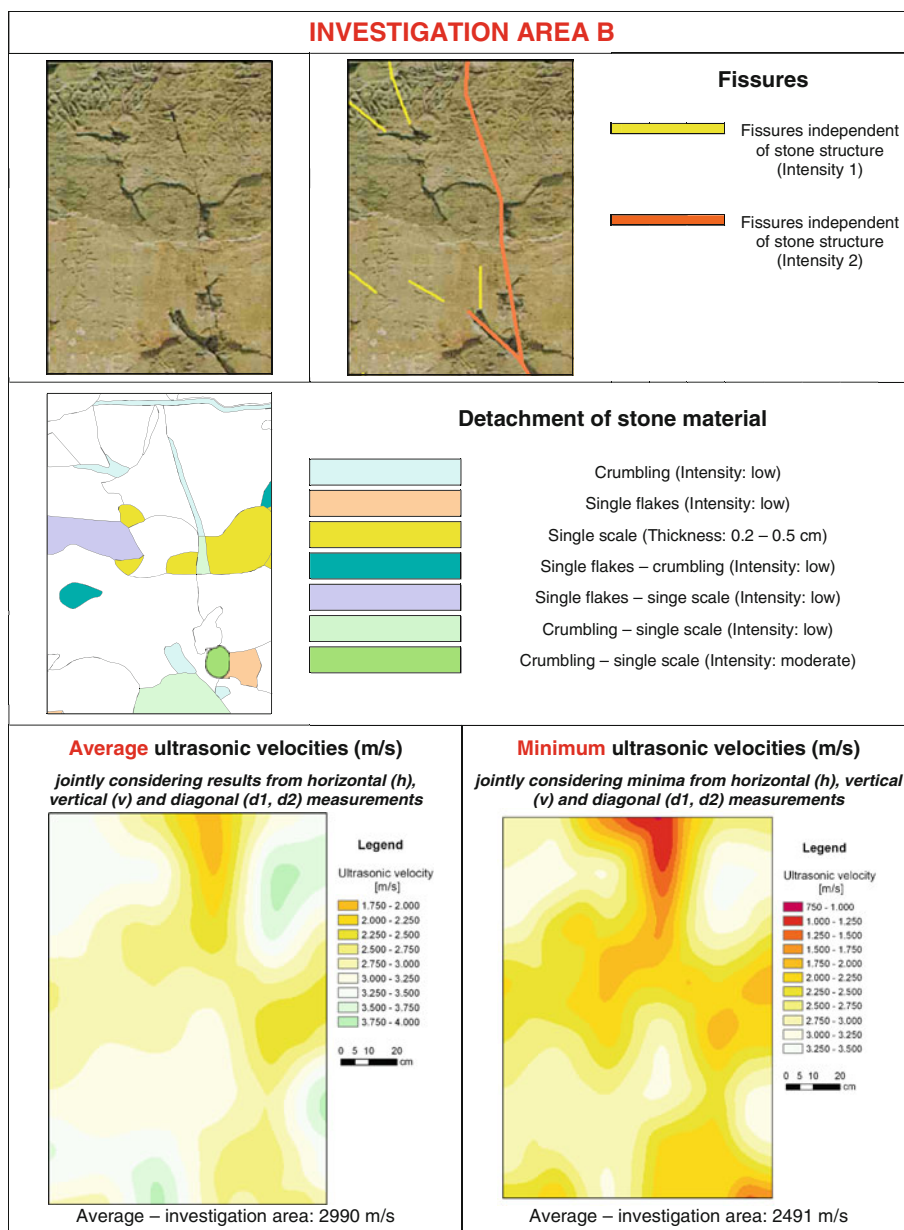
Weathering forms were used for the assessment of weathering damage according to phenomenological criteria. More than 300 partial areas of the monument's surface were distinguished in the course of monument mapping as a result of different types, intensities and combinations of weathering forms concerning loss of stone material, discolouration/deposits on the stone surface, current detachment of stone material and fissures. This reveals the rather complex weathering state of the monument that has to be faced. Two-thirds of the monument's stone surface have already suffered loss of stone material. More than 40% of the stone surface are currently affected by detachment of

stone material, especially by crumbly disintegration and contour scaling. In addition, the state of the monument is characterized by a rather dense network of fissures.

Based on the findings relating to discolouration/deposits, current detachment of stone material and loss of stone material, four phases can be deduced with respect to weathering progression (Fig. 30):

- Phase I, earliest phase: The stone surface is not affected by detachment/loss of stone material until now. Today, only discolouration/deposits are found on the stone surface. 25.4% of the monument are concerned, mainly limited to the lower part of the rock face (with exception of the lowermost margin).

**Fig. 23** Investigation area B: maps of average and minimum ultrasonic velocities. In addition, corresponding maps of fissures and weathering forms relating to current detachment of stone material



- Phase II: The stone surface is affected by detachment of stone material (first generation of detachment), however, has not suffered loss of stone material yet. In addition, discolouration/deposits occur. Only 10.1% of the monument are concerned (irregular distribution).
- Phase III: The stone surface has suffered loss of stone material as a result of prior detachment of stone material (phase II). In addition, discolouration/deposits occur. The stone surface is not affected by further detachment of stone material. About one-third of the monument's surface—mainly limited to the upper part of the monument (with exception of the uppermost

margin)—has entered this phase of weathering progression.

- Phase IV: After having suffered loss of stone material, the surface is again affected by detachment of stone material. In addition, discolouration/deposits occur. Another one-third of the monument's surface has entered this most proceeded phase of weathering progression (upper part, lowermost part, irregular distribution in the central part).

Thus, two-thirds of the monument's stone surface have already entered advanced phases III and IV of weathering progression.



**Fig. 24** Correlation scheme “weathering forms–damage categories”

LOSS OF STONE MATERIAL						
<i>Back weathering due to loss of scales (sW) or due to loss of crumbs (uW)</i> <i>Rounding / notching (Ro)</i> <i>Weathering out dependent on stone structure (tR)</i>	Intensities	Depth (cm)				
	Damage categories	0.2	0.2 - 0.5	0.5 - 1	1 - 2	2 - 5
<i>Break out due to natural cause (nO)</i>	Intensities	Volume (cm <sup>3</sup> )				
	Damage categories	5	5 - 50	50 - 500	500 - 1000	1000 - 2500
DISCOLOURATION / DEPOSITS						
<i>Colouration (Dc)</i> <i>Microbiological colonization (Bi)</i>	Intensities	Colouration: degree – change of colour Microbiological colonization: degree – covering of the surface				
	Damage categories	low		high		
<i>Soiling by particles from the atmosphere or from water (wl)</i> <i>Coloured crust tracing the surface (fkC)</i>	Intensities	no differentiation of intensities				
	Damage category	1				
DETACHMENT OF STONE MATERIAL						
<i>Crumbling (Pu)</i>	Intensities	Mass of detaching stone material				
	Damage categories	low	moderate	high		
<i>Single scale (eS)</i> <i>Multiple scales (mS)</i>	Intensities	Thickness of the scale / stack of scales (cm)				
	Damage categories	0.2	0.2 - 0.5	0.5 - 1	1 - 2	2 - 3
<i>Splitting up (Xv)</i>	Intensities	Number of detaching stone layers resp. splits				
	Damage categories	low		high		
<i>Single flakes to crumbling (eF-Pu)</i> <i>Crumbling to single scale (Pu-eS)</i>	Intensities	Mass of detaching stone material				
	Damage categories	low	moderate	high		
<i>Single flakes (eF)</i> <i>Multiple flakes (mF)</i> <i>Single flakes to single scale (eF-eS)</i> <i>Multiple flakes to multiple scales (mF-mS)</i>	Intensities	Mass of detaching stone material				
	Damage categories	low	moderate	High		
DAMAGE CATEGORIES						
0	1	2	3	4	5	
no damage	very slight damage	slight damage	moderate damage	severe damage	very severe damage	

Profile measurements were carried out at 30 petroglyphs of the Bronze Age for quantifying the morphological profile of the carvings. The results show that the high historical and cultural importance of the Cheonjeon-ri monument is limited to an outermost stone surface zone of only few millimetres in case of the Bronze Age carvings. Based on the quantitative evaluation of the surface profiles, a quantitative risk prognosis—% of carvings completely lost in dependence upon future recession of the stone surface—was derived for the Bronze Age carvings (Fig. 31). For example, if the stone surface was to recede 5 mm, at least 33% of the carvings would be lost. If it was to recede 7 mm, almost 80% of the carvings would be completely

lost. This means that even slightest erosion will result in the disappearance of carvings. This prognosis is quite alarming. With respect to the carvings of the Silla Period, it can be stated that their profile depths are even lower than those of the Bronze Age carvings. This means that risk prognosis for these younger carvings would turn out to be even more alarming.

With respect to results obtained from rebound hardness measurements and ultrasonic measurements, it was found that high rebound hardnesses and ultrasonic velocities reflect a high compactness/hardness of the stone material when not affected by disintegration. Low rebound hardnesses reveal intense detachment of stone material. The

		Damage categories for discolouration / deposits			0	1	2
		0	1	2			
Damage categories for loss of stone material	0	<i>0</i>	<i>1</i>	<i>2</i>	0	1	2
		<i>2</i>	<i>2</i>	<i>2</i>	2	2	2
		<i>3</i>	<i>3</i>	<i>3</i>	3	3	3
		<i>4</i>	<i>4</i>	<i>4</i>	4	4	4
		<i>5</i>	<i>5</i>	<i>5</i>	5	5	5
	2	<i>2</i>	<i>2</i>	<i>2</i>	0	2	2
		<i>3</i>	<i>3</i>	<i>3</i>	2	3	3
		<i>4</i>	<i>4</i>	<i>4</i>	3	4	4
		<i>5</i>	<i>5</i>	<i>5</i>	4	5	5
		<i>3</i>	<i>3</i>	<i>3</i>	5	3	3
	3	<i>3</i>	<i>3</i>	<i>3</i>	2	3	3
		<i>3</i>	<i>3</i>	<i>3</i>	3	3	3
		<i>4</i>	<i>4</i>	<i>4</i>	4	4	4
		<i>5</i>	<i>5</i>	<i>5</i>	5	5	5
		<i>4</i>	<i>4</i>	<i>4</i>	0	4	4
4	<i>4</i>	<i>4</i>	<i>4</i>	2	4	4	
	<i>4</i>	<i>4</i>	<i>4</i>	3	4	4	
	<i>5</i>	<i>5</i>	<i>5</i>	4	5	5	
	<i>5</i>	<i>5</i>	<i>5</i>	5	5	5	
	<i>5</i>	<i>5</i>	<i>5</i>	0	5	5	
5	<i>5</i>	<i>5</i>	<i>5</i>	2	5	5	
	<i>5</i>	<i>5</i>	<i>5</i>	3	5	5	
	<i>5</i>	<i>5</i>	<i>5</i>	4	5	5	
	<i>5</i>	<i>5</i>	<i>5</i>	5	5	5	
	<i>5</i>	<i>5</i>	<i>5</i>	5	5	5	

**Fig. 25** Scheme for the determination of final damage categories (*italic, bold numbers*) jointly considering loss of stone material, discolouration/deposits and detachment of stone material

**DAMAGE INDEX**

$$DI = \frac{(A \cdot 0) + (B \cdot 1) + (C \cdot 2) + (D \cdot 3) + (E \cdot 4) + (F \cdot 5)}{100} = \frac{B + (C \cdot 2) + (D \cdot 3) + (E \cdot 4) + (F \cdot 5)}{100}$$

A = Area (%) – damage category 0      D = Area (%) – damage category 3  
 B = Area (%) – damage category 1      E = Area (%) – damage category 4  
 C = Area (%) – damage category 2      F = Area (%) – damage category 5

$$\sum_A^F = 100 \quad 0 \leq DI \leq 5$$

**Fig. 26** Calculation of the damage index

fact that the rebound hardness determined for the carved areas (petroglyphs) without any visible stone deterioration is significantly lower compared to non-carved areas without any visible loss and current detachment of stone material may indicate a weakening of stone fabric due to the carving procedure (mechanical impact). This finding displays the carved parts as more sensitive to future weathering than non-carved parts. Low ultrasonic velocities reflect the network of fissures and intense current detachment of stone material.

With respect to results obtained from ultrasonic measurements, the maps “minimum ultrasonic velocities”

reflect the maximum extent of weathering damage. With ultrasonic velocities of 2,085 m/s (investigation area A) and 2,491 m/s (investigation area B) on average, they indicate considerable stone disintegration and/or structural discontinuities.

With respect to evaluation of weathering damage by means of damage categories and damage indices, it was found that two-thirds of the monument’s stone surface are already affected by severe or even very severe damage, if jointly considering loss of stone material, discolouration/deposits and current detachment of stone material. The overall damage index for the monument amounts to 3.57. This is alarming, considering that the damage index can only range between 0 and 5.0 as per definition.

By trend, the vertical profiles of damage indices show higher damage indices for the upper part of the monument (with carvings of the Bronze Age) relating to loss of stone material, detachment of stone material and total damage, whereas higher damage indices are stated for the lower part of the monument (with carvings of the Silla Period) with respect to discolouration/deposits.

With respect to phases I–IV of weathering progression mentioned before, following damage indices were determined:

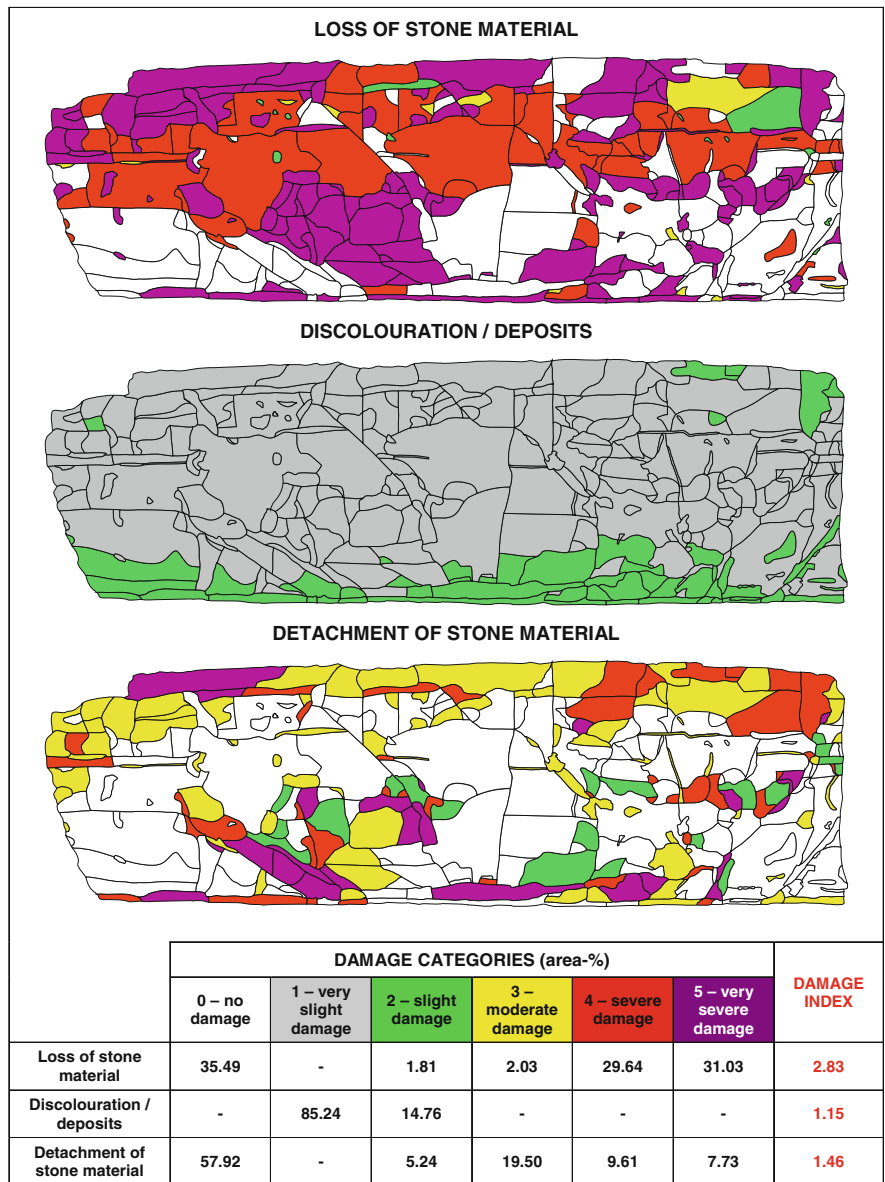
- stone surface attributed to phase I (stone surface not affected by detachment/loss of stone material until now), damage index: 1.20.
- stone surface attributed to phase II (stone surface affected by detachment of stone material, however, no loss of stone material until now), damage index: 3.90.
- stone surface attributed to phase III (stone surface affected by loss of stone material, currently no further detachment of stone material), damage index: 4.17.
- stone surface attributed to phase IV (after having suffered loss of stone material again affected by detachment of stone material), damage index: 4.75.

The fact that two-thirds of the monument’s stone surface have already entered advanced phases III and IV of weathering progression—characterized by very high damage indices—is alarming.

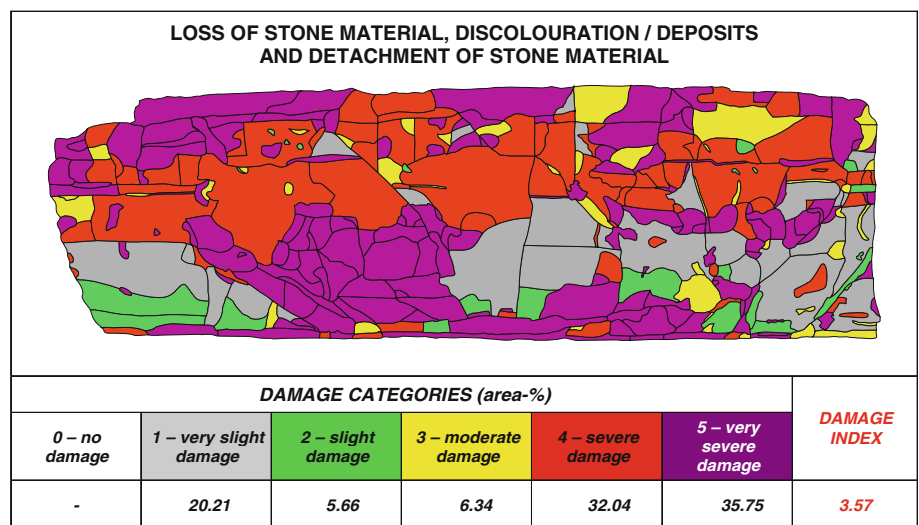
**Conclusions**

Systematic diagnostical studies were carried out for the assessment of weathering damage on the Petroglyphs of Cheonjeon-ri in Ulsan/Republic of Korea. Assuming that carvings once were distributed all over the surface of the monument, it can be stated in summary that a considerable part of the carved surface is already irretrievably lost. Many of the remaining petroglyphs show reduced profile depths, which is considered as a result of erosion provoked

**Fig. 27** Maps of damage categories relating to loss of stone material, discolouration/ deposits and detachment of stone material, quantitative evaluation of damage categories with determination of the damage index



**Fig. 28** Map of final damage categories jointly considering loss of stone material, discolouration/deposits and detachment of stone material, quantitative evaluation of damage categories with determination of the damage index



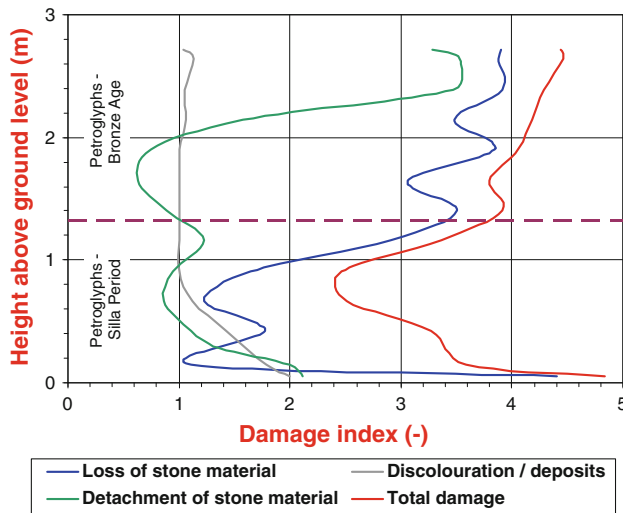


Fig. 29 Zonation of damage: vertical damage index profiles

by non-visible detachment of finest stone particles. Several parts of the stone surface with carvings currently are affected by detachment of stone material, which displays the danger of further irretrievable loss of cultural heritage. In addition, the rather dense network of fissures bears the risk of structural instability and the break out of further stone fragments. Furthermore, the fissures have to be considered as additional paths for water uptake and water migration. Considering considerable reductions in rebound hardness and ultrasonic velocity values and results on damage categories and damage indices, an alarming extent of damage is revealed. The considerable threat to the historical site of Cheonjeon-ri due to weathering—outlined by

Fig. 30 Map relating to phases I–IV of weathering progression with quantitative evaluation (area%)

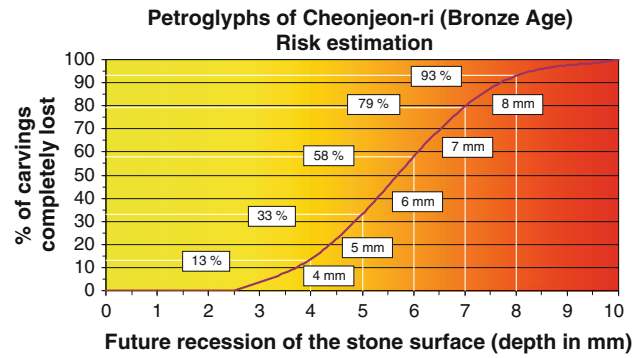
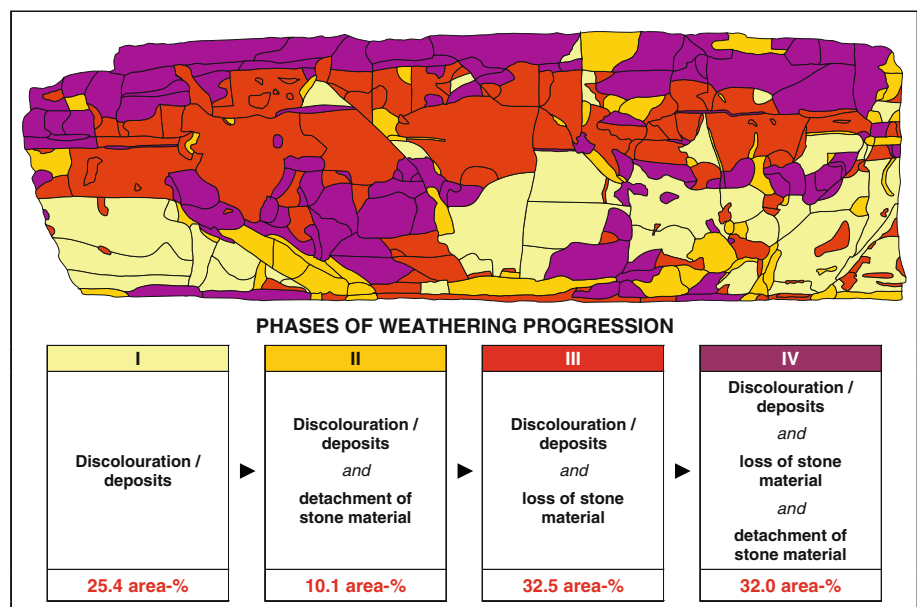


Fig. 31 Risk prognosis derived from profile measurements at carvings of the Bronze Age

the results of the diagnostical studies—indicates the need of intervention for monument preservation. Decision of appropriate preservation strategies—including immediate safeguarding measures, measures for the reduction of causes of damage, measures for remedy of damage, preventive measures—will necessitate supplementary information from other disciplines such as rock mechanics, hydrology/hydrogeology, climatology, engineering sciences, microbiology, etc. At present, the continuous monitoring of the monument is highly recommended in order to recognize any further increase of weathering damage at the earliest possible stage and to eventually initiate immediate intervention.

**Acknowledgments** The authors would like to express their gratitude to the authorities of Ulsan Metropolitan City for their support of the studies on the Petroglyphs of Cheonjeon-ri.

## References

- Cultural Heritage Administration of Korea. <http://www.ocp.go.kr>
- Fitzner B, Heinrichs K (2002) Damage diagnosis on stone monuments—weathering forms, damage categories and damage indices. In: Prikryl R, Viles H (eds) *Understanding and managing stone decay*. Proceedings of the international conference on stone weathering and atmospheric pollution network (SWAPNET 2001). Charles University, Karolinum Press, Prague, pp 11–56
- Fitzner B, Heinrichs K, La Bouchardiere D (2002) Damage index for stone monuments. In: Galan E, Zezza F (eds) *Protection and conservation of the cultural heritage of the Mediterranean cities*. Proceedings of the 5th international symposium on the conservation of monuments in the Mediterranean basin, Sevilla, Spain, 5–8 April 2000. Swets & Zeitlinger, Lisse, The Netherlands, pp 315–326
- Fitzner B, Heinrichs K, La Bouchardiere D (2004) The Bangudae Petroglyph in Ulsan, Korea: studies on weathering damage and risk prognosis. *Environ Geol* 46:504–526
- Heinrichs K (2008) Diagnosis of weathering damage on rock-cut monuments in Petra, Jordan. *Environ Geol* 56:643–675. doi:10.1007/s00254-008-1358-1
- Heinrichs K, Fitzner B (2007) Stone monuments of the Nemrud Dag sanctuary/Turkey—petrographical investigation and diagnosis of weathering damage. *Z dt Ges Geowiss* 158(3):519–548, E. Schweizerbart'sche Verlagsbuchhandlung, Stuttgart. doi:10.1127/1860-1804/2007/0158-0519
- Hirschwald J (1908) *Die Prüfung der natürlichen Bausteine auf ihre Wetterbeständigkeit*. Verlag von Wilhelm Ernst & Sohn, Berlin
- Kim SJ (ed) (2002) *Proceedings of the international symposium on the conservation of the Bangudae Petroglyph*. Stone Conservation Science Laboratory, Ulsan City
- Kownatzki K (1997) *Verwitterungszustandserfassung von Natursteinbauwerken unter besonderer Berücksichtigung phänomenologischer Verfahren*. Diss. RWTH Aachen, Aachener Geowiss. Beiträge, 22, Augustinus, Aachen
- Mottershead D (2000) Identification and mapping of rock weathering surface forms and features. *Zeit Geomorph NF Supp Bd* 120:5–22
- Nappi A, Côte P (1997) Nondestructive test methods applicable to historic stone structures. In: Baer NS, Snethlage R (eds) *Saving our architectural heritage—the conservation of historic stone structures*. Dahlem Workshop Report. John Wiley & Sons, Chichester, England, pp 151–166
- Pettijohn FJ, Potter PE, Siever R (1987) *Sand and sandstone*, 2nd edn. Springer, Berlin
- Prikryl R (2007) Understanding the Earth scientist's role in the pre-restoration research of monuments: an overview. In: Prikryl R, Smith BJ (eds) *Building stone decay: from diagnosis to conservation*. Geological Society, Special Publications, London
- Smith BJ, Whalley WB, Magee RW (1992) Assessment of building stone decay: a geomorphological approach. In: Webster RGM (ed) *Stone cleaning and the nature. Soiling and decay mechanisms of stone*. Donhead Publishing, London, pp 249–257
- Snethlage R (2005) *Leitfaden Steinkonservierung*. Fraunhofer IRB, Stuttgart
- Tucker M (1988) *Techniques in sedimentology*. Blackwell Scientific Publications, Oxford
- Van der Sluijs MA. Korea's prehistoric past. Online publication: <http://www.mythopedia.info/prehistoric-Korea.pdf>
- Yim S. Petroglyphs of Korea. Online publication: <http://anu.andong.ac.kr/~yimsk/petroglyphs/petro-eng/petro-eng.html>